3 Microscopic description of traffic phases

The previous chapter has shown that the description of the driving strategy of a vehicle of most of the present models is based on first principles and that the models fail to give a detailed description of all of the traffic states. Unfortunately, although in the last few years several empirical studies that have been carried out were motivated by the aim of obtaining a more profound picture of highway traffic, not much is known about the behavior of single vehicles. It is therefore indispensable to improve the understanding of the microscopic driving behavior of the vehicles in the various traffic states in order to allow a more realistic and detailed reproduction of the vehicle movement.
In this chapter a detailed analysis of single-vehicle data is presented that sheds some light on the microscopic interaction of the vehicles and helps to validate the properties of models for traffic flow on a qualitative level (see chapter 4). It is worth pointing out that the data set underlying the study is one of the largest used so far. In contrast to earlier studies the data have been collected on a 3-lane road without speed limit and relatively (several kilometers) far away from ramps which allows a comparison with idealized traffic simulations. The quality of the empirical data enables a detailed insight into the dynamics of the vehicles in wide jams. The results are therefore of direct relevance for the modeling of traffic flow on highways. Also some open questions concerning the time-headway distribution will be resolved.
The analysis of single-vehicle data gives important information about the driving behavior of the vehicles in the various traffic states [1]. Unfortunately, up to now only a few empirical results of single-vehicle data exist [110, 133] (see section 2.2.2) that do not provide a consistent picture of the vehicle dynamics. It was shown that the distribution of the time-headways and the velocity-distance relationship do not depend on the density but on the traffic state. In [110] a peak at 1.8 s was found in the time-headway distribution that was explained with the drivers' effort for safety. However, the existence of this peak could not be confirmed in [133]. Moreover, in the free flow state platoons of vehicles driving bumper-to-bumper with a time-headway well below 1 s occur.
The velocity-distance relationship provides information on the adjustment of the velocity on the headway. While in free flow the velocity shows large values even for small headways, in the congested state drivers tend to move slower than the distance allows. Thus, in the free flow regime the movement of the vehicles is uncorrelated although small platoons exist, while in the synchronized regime large correlations of the velocity between the vehicles can be found. Despite the correlations the distance between the vehicles can vary considerably.

3.1 Empirical data

The data sets were collected at different locations on two highways in North-Rhine-Westfalia, Germany. The first set is provided by two detectors, one for each driving

[1] In order to identify the different phases it would be ideal to have data from a series of detectors that allows to characterize the traffic states by their spatio-temporal properties [73]. Since this is not possible, the autocorrelation and cross-correlation functions are used to determine these properties locally.

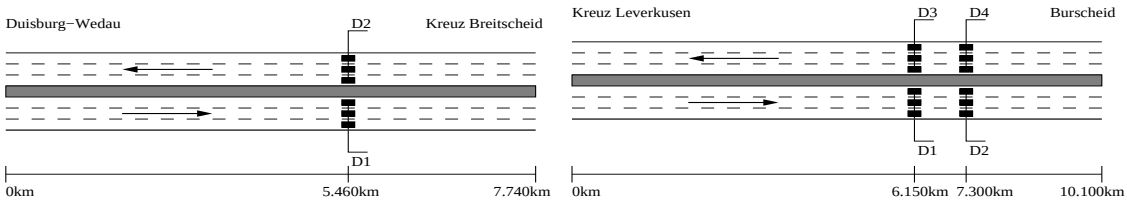

Figure 3.1: Location of the detectors of the first data set (left) measured on the A3 near Duisburg and of the second and third data set (right) measured on the A1 near Leverkusen.

direction, on the A3 between the junction Duisburg-Wedau and the highway-intersection Kreuz-Breitscheid (see Fig. 3.1). A detector consists of three inductive loops, one for each lane. The location of the detector is about 5.5 km from the highway intersection Breitscheid and about 2.2 km from the junction Duisburg-Wedau. It is important to note that there is no speed limit. The data set was measured between 03-30-2000 and 05-16-2000 and comprises 48 days. The second and the third data set was measured by four detectors, one for each driving direction consisting of three inductive loops, at two locations on the A1 between the highway intersection Leverkusen and the junction Burscheid (see Fig. 3.1). Note that for storage reasons, in the third data set only the vehicles on the right and the middle lane were detected. The detectors are located at 6.150 km, respectively 7.300 km from Leverkusen, and at 3.950 km, respectively 2.800 km from Burscheid, with a distance of 1.150 km between the two measurement locations. The data were collected during two periods (08-02-2000 to 08-20-2000 and 02-01-2001 to 02-27-2001) which comprises a total measurement time of 46 days. Note that the highway has three lanes and that there is no speed limit. In total were measured about 9.5 million cars on 94 days.
All of the inductive loops were able to measure single-vehicle data. A data set of one vehicle comprises the time (in hundredth seconds) at which the vehicle reaches the detector, the lane the car is detected, the type of the vehicle (car, truck), the velocity in km/h and its length in cm. The length of a vehicle is calculated with an accuracy of 1 cm. The lower bound for the velocity measurement is 10 km/h, i.e., velocities of slower vehicles are not measured. Then, instead of the length of the vehicle, the time the inductive loop is covered with a vehicle is given in hundredth seconds. Note that the velocity is theoretically calculated internally via the time dt a vehicle needs to pass a detector of a given length with an accuracy of 1 km/h. However, since dt is only measured in milliseconds and no floating points for the calculation of the velocity are used, it is possible that a velocity may correspond to more than one dt, and/or a difference of one millisecond in dt leads to a velocity difference larger than 1 km/h. As a result, small differences in dt cannot be resolved while some velocities cannot be measured.
The third data set includes the electric signal inducted in the loops when a car passes the detector. These data comprise the time (in milliseconds) at which the vehicle arrives at the detector and the time-series of the height of the electric signal that is sampled at 125 points in one second.
In addition to the single-vehicle data of the first and the second data set, one minute averages of the traffic data are collected. These data comprise the number of cars and the number of trucks, the mean velocity of cars, the mean velocity of trucks and the mean velocity of all vehicles. The density is estimated by occupancy. It is simply given by the percentage of time the detector is covered by a vehicle. Throughout this chapter the

terminology "density" is used for occupancy if not stated otherwise, and the occupancy is calculated in percent.
Since large occupancies (e.g., a vehicle blocks the detector for more than one minute) are not distributed on minute intervals by the counting device, but the occupancy is just related to the interval the vehicle is measured, a cut-off of the minute averaged data at 100 % was introduced. Thus, the explicit calculation of the occupancy by means of the single-vehicle data via equation (2.7) allows to determine the occupancy more accurately compared to the one minute data because occupancy overlaps from minute to minute can be considered. The minute data therefore are only used to verify the averaged single-vehicle data.
The time resolution of the single-vehicle data allows the calculation of the time-headway t_n^h and the distance-headway d_n of the n-th vehicle via equation (2.4) and equation (2.5). Because of the resolution of the internal clock (hundredth seconds) the time-headway can be calculated with an accuracy of 0.01 s and the distance-headway with an accuracy of 1 cm.
In order to allow the calculation of spatio-temporal correlations on the A1, the two measurement locations D3/D4 and D2/D4 are synchronized by means of radio controlled clocks.
Distribution functions $P(x)$ of the observable x with the discretization Δx that are obtained from the empirical data have been normalized such that $\sum P(x) \cdot \Delta x = 1$. This guarantees that the distributions are independent from the binning of the data.

3.2 Free flow

Free flow is the traffic state most frequently observed in the data set and characterized by a large flow J and velocity v and a small density (Fig. 3.2). While daily variations of the flow and the density become visible in the time-series[2], the velocity remains nearly constant over the whole day.
Due to legal restrictions in Germany, vehicles have to drive on the right lane, and the left and the middle lane should be used only for overtake maneuvers. Thus, the lanes segregate into fast and slow lanes which results in a negative velocity gradient from left to right (Fig. 3.2). This effect becomes more pronounced in the absence of a speed limit. As a consequence, the flow and the velocity decrease from the left to the right lane, whereas the density increases.
Next, the velocity distributions in free flow traffic are analyzed (Fig. 3.3). The velocity calculated by the detector is simply the length of the detector divided by the passing time dt, which is measured directly. Here, dt is measured with a precision of milliseconds, but the corresponding velocity is given in units of km/h since only integer arithmetics was applied internally. This way of calculating the velocity does not use the full precision of the measurement, but even worse it leads to an uneven sampling of the velocities.
The latter point can be avoided by recovering the corresponding traveling time dt from the velocity given in the data set. For large velocities ($v > 110$ km/h) a unique value of dt is obtained, for smaller velocities, however, each velocity corresponds to a range of possible traveling times. If the same velocity results in k different traveling times, the statistical weight of each possible value of dt is simply increased by $1/k$. Finally, the corrected velocity distribution is recalculated by using the precise values of the velocities for a given value of dt. This procedure leads obviously to very smooth velocity distributions.

[2]Quantitatively they can be seen in the behavior of the autocorrelation functions [110].

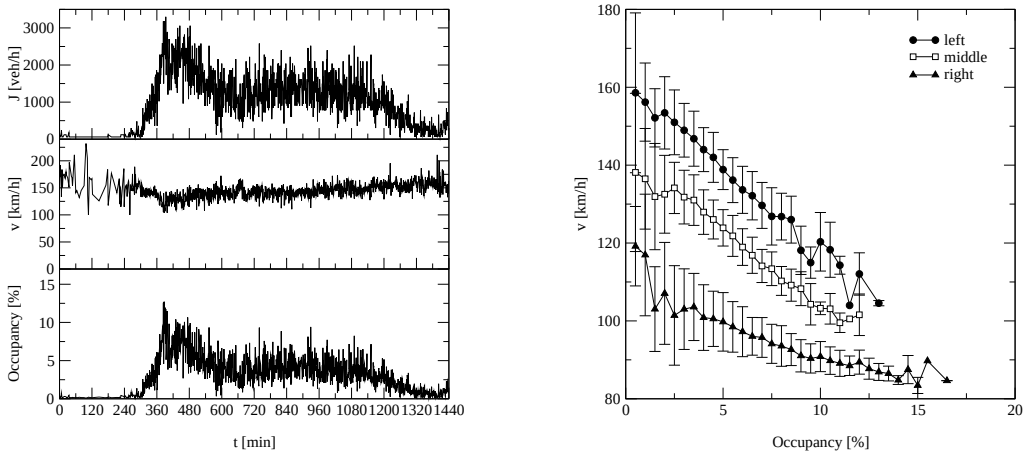

Figure 3.2: Time-series in the free flow regime of the flow, the velocity and the occupancy on the left lane (left) and average velocity versus the density for the three lanes (right) at detector D1 on the A3 on the 04-28-2000.

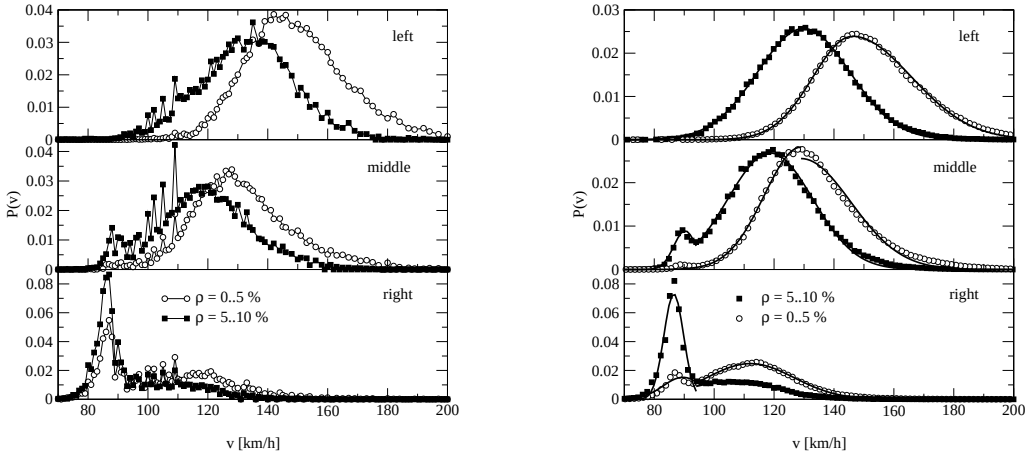

Figure 3.3: Distribution of the velocity on the three lanes (left) and with correction of the rounding errors (right, see text) at detector D1 on the A3 on the 04-28-2000. The solid lines represents best fits with distributions of Gaussian type.

On the left lane the velocity distributions can be nicely fitted to a Gaussian distribution, for densities between $5-10\%$. This is in agreement with earlier investigations, also finding Gaussian distributed velocities, for a low portion of trucks [40]. For lower densities ($0-5\%$), however, a slight asymmetry of the distribution function is observed. In order to quantify this asymmetry, the distribution function is divided into two parts, one containing all velocities below the maximum of the distribution, and the other for larger velocities. Both

density	distribution	a	b	c
$0-5\%$	left, $v < 146$ km/h	146.0	340.79	41.93
	left, $v \geq 146$ km/h	146.0	788.98	41.80
	middle, $v < 129$ km/h	129.0	300.21	35.46
	middle, $v \geq 129$ km/h	129.0	556.74	39.12
	right, cars	112.10	424.22	40.40
	right, trucks	89.55	88.44	65.70
$5-10\%$	left	129.9	477.84	38.92
	middle, cars	118.75	401.50	37.27
	middle, trucks	90.27	28.10	112.27
	right, cars	106.24	466.06	80.95
	right, trucks	86.51	21.72	13.69

Table 3.1: Fit parameters of the velocity distribution in free flow. As fit function the Gaussian $p(v) = \exp(-(v-a)^2/b)/c$ was used.

parts are in agreement with different Gaussian distributions (Fig. 3.3).
The form of the distribution function on the middle and on the right lane is different because they can be used by trucks. The trucks lead to a second maximum of the velocity distribution. For these lanes, the velocity distribution can be viewed as a superposition of a "car"and a "truck" velocity distribution, both of Gaussian form in the density interval $5-10\%$. For lower densities, again, a slight asymmetry of the distribution function is observed. For an overview, the parameters of the distributions are summarized in table 3.1.
In the presence of a speed limit it was found that the negligible vehicle interactions are one of the main characteristics of free flow traffic [110]. In contrast, the velocity-density relationship in Fig. 3.4 clearly deviates from a constant value. This fact can be explained by the absence of a speed limit. Slow vehicles are responsible for the decrement of the mean velocity with increasing density. The average velocity decreases linearly with the occupancy ($v \approx 160.206 \pm 0.4884 - (4.44036 \pm 0.1169)occ$) and consequently the flow quadratically, $J \approx 5.02139 \pm 4.334 + (368.543 \pm 2.177)occ - (9.54743 \pm 0.2377)occ^2$. In contrast, queuing theory predicts for a M/G/2 queuing system that has to be applied for a three-lane highway [97] a quadratic relationship between density and velocity and a cubic relationship between density and flow, respectively. For two-lane highways (a M/G/1 queuing system), the velocity is expected to depend linearly on the density. The discrepancy between queuing theory and empirical data may indicate that either the theory is not appropriate or that the three lanes are not homogeneously coupled. The latter point of view is supported by a correlation analysis of the different lanes, showing that the coupling between left and middle lane is much stronger than between the right and middle lane. It would be interesting to parameterize the partial decoupling of the right lane and to study the modified queuing theory.
The velocity-headway curve illustrates the velocity adjustment of the vehicles on the distance-headway. Since cars can move freely, the velocity saturates even for small distances. However, with increasing vehicle interaction the asymptotic value of the velocity decreases (Fig. 3.4).
The vehicle interactions, although visible in the fundamental diagram, are very small. In Fig. 3.5 the autocorrelation (see appendix A) of the one-minute averages of the velocity is represented. In order to eliminate the daily variations the time-series of the velocity was

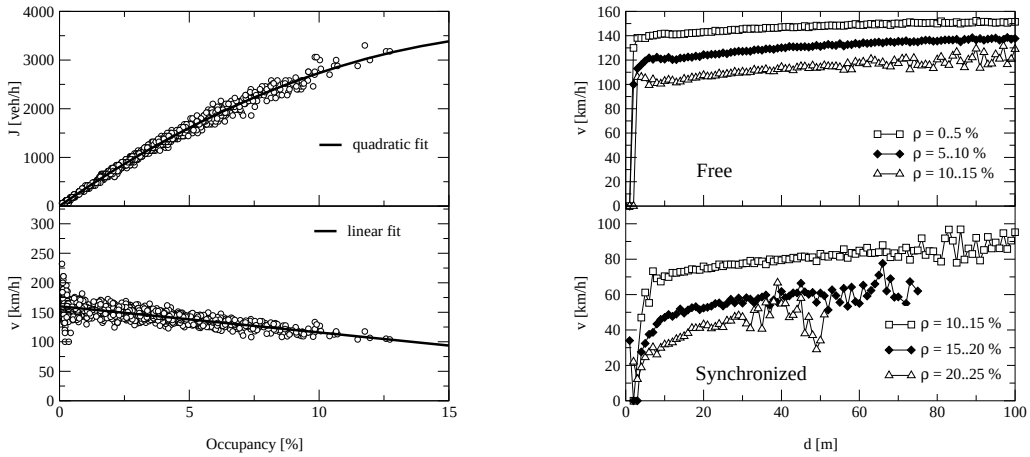

Figure 3.4: Left: Fundamental diagram of the left lane for the flow and the velocity in the free flow regime on the 04-28-2000 at detector D1 on the A3. The solid curve gives the best fit for the data. Right: The mean velocity chosen for a certain distance-headway at detector D1 on the left lane of the A3 for all days with free flow and synchronized traffic.

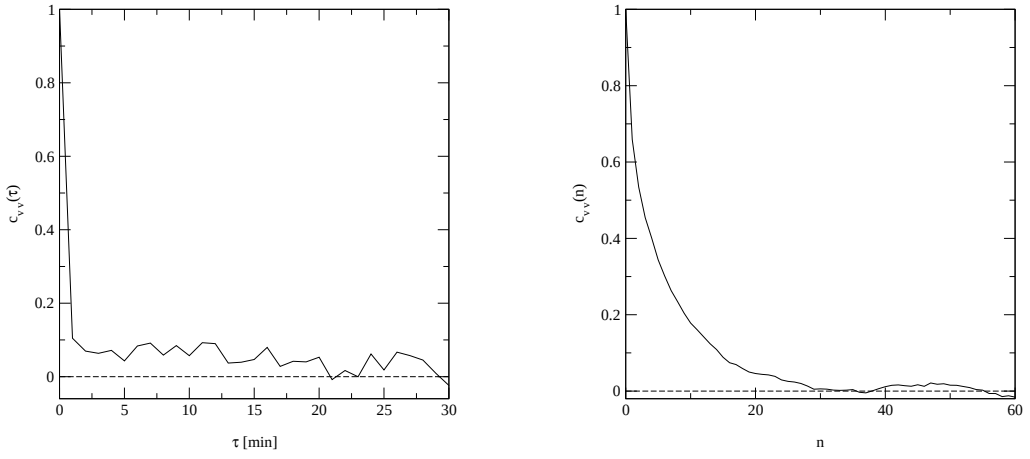

Figure 3.5: Autocorrelation of the minute averaged velocity (left) and of the single-vehicle velocity (right) in free flow of the left lane at detector D1 on the 04-28-2000 on the A3.

detrended[3] by a linear fit. Obviously, the minute averaged velocity shows no correlations on time scales larger than one minute, since the vehicles are in general driving independently. Nevertheless, a closer look on the autocorrelation of the velocity of the single-vehicle data

[3]The data were fitted using a linear regression. This trend was then subtracted from the data points.

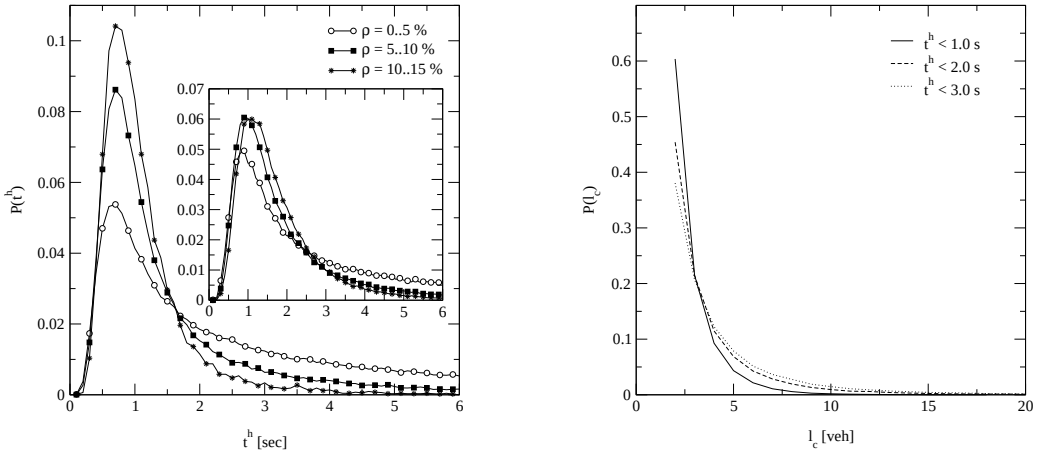

Figure 3.6: Left: Distribution of the time-headways of the left lane at detector D1 on the A3 for all days of the data set with free flow. The inset shows the time-headway distribution of new measurements on the A1 near Köln-Lövenich. Right: Cluster length distribution in the free flow regime for different time-headways at detector D1 on the A3 on the 04-28-2000 on the left lane.

(Fig. 3.5) reveals correlations on very short time-scales. Like the minute-averaged data, the single-vehicle data were detrended to eliminate daily variations. Now, the autocorrelation function is not time-dependent but depends on the number of vehicles. The strong correlations on short time-scales can be attributed to small platoons of cars driving with nearly the same speed but with very small headways [110]. The platoons are also responsible for small time-headways in the time-headway distribution (Fig. 3.6). As one can see from Fig. 3.6, the time-headway distribution differs from the distribution found in [110]. In [110] the time-headway distribution of the single-vehicle data shows the existence of a peak at 1.8 s for all densities and all traffic states which was explained to be the optimal safe time-headway between vehicles.
This peak was missing in related empirical investigations [133] including the present. In order to clarify the origin of this peak, the data used in [110] was analyzed again. A detailed analysis of this data set revealed even more than one peak, but also smaller peaks for other multiples of 0.9 s. Therefore one is let to the believe that these peaks could be artificially generated by a software error of the detection device. Indeed it turned out that in case of a busy detector the data are not directly transfered but stored in a buffer for a time of 0.9 s. Since the single-vehicle data contain no time-stamp and the storage time of the internal clock of the computer was used, to each data point in the buffer the same time of measurement is assigned. In the time-headway distribution then the multiples of the buffer size become visible. This is confirmed by new measurements (see inset of Fig. 3.6) at the detectors D2 and D3 on the A1 near Köln-Lövenich that have also been used in [110]. This data set (like the data sets used in this paper) records the time when a vehicle arrives at the detector in hundredth seconds which therefore allows the calculation of the exact time-headway. The new data do not show a peak at 1.8 s in the time-headway distribution (about 1.5 million cars were detected in 19 days).

At this point it is stressed that the velocity and length measurements of the single-vehicle data of [110] are not affected by the software error and, more important, that the order of the data is not mixed up. In particular, results of the fundamental diagram, the time-series analysis and the optimal-velocity curve can be reproduced by the data sets used here.
The time-headway distribution found here shows a strong dependence on the density. However, although the width of the distribution decreases, the short time behavior remains nearly unchanged. Not only the maximum of the distribution is at about 0.68 s, but also the values of the shortest time-headways do not change significantly. Note that the distribution was calculated by considering all days of the data set with free flow traffic. If one compares the time-headway distributions of the highway with and without speed limit, one observes that, in case of an applied speed limit, the maximum of the distribution is shifted towards larger time-headways. This observation underlines the importance of anticipation effects in free flow traffic. However, the anticipation of the predecessor's movement leads to serious problems concerning safe driving because the drivers adjust the distance to the leading vehicle discarding their own velocity.
Another important point is the cut-off of the distribution at small time-headways. In both cases it is found that a non-negligible portion of vehicles drives with a temporal distance of the order ~ 0.2 s, that is comparable to the reaction time of the drivers. These drivers take a very high risk to provoke an accident and would definitively be unable to avoid a crash in case of a sudden obstacle.
It is now possible to estimate the temporal extension of the platoons. From the decay of the autocorrelation of the single-vehicle velocity follows a platoon length of the order of magnitude of about 10 vehicles. Since the time-headways within a platoon are smaller than the maximum of the distribution (about 1 s), this leads to values less than one minute. Thus, these small vehicle clusters cannot be visible in the minute averaged data.
The analysis of the single-vehicle data allows to measure cluster lengths directly. A platoon of the length l_c consists of l_c consecutive vehicles, each having a time-headway smaller than a defined value[4]. By counting the number of succeeding vehicles with time-headways well below a certain value, one obtains the cluster length distribution (see Fig. 3.6 for the distribution of the left lane). The length of the platoons increases with increasing time-headway, but even with very small time-headways lengths up to 14 vehicles can be measured. In contrast to vehicles on the middle and the right lane, cars on the left lane have no possibility to overtake a slower one. As the length of the platoons decreases from the left to the right lane, one can conclude that platoons are simply formed by fast cars piling up behind a slow car (see [58] for a functional relationship of the bunch size distribution).
Driving bumper-to-bumper with large velocity requires an increased attention to velocity fluctuations of the preceding vehicle. As a consequence, the velocity of vehicles inside a platoon is almost synchronized. This fact leads to a slow decay of the autocorrelation function. Driving in a synchronized manner also decreases the velocity differences within the platoon. In Fig. 3.7 the standard deviation of the velocity of all platoon vehicles is depicted. As one can see, the smaller the time-headway, the smaller the velocity differences. Furthermore, the standard deviation saturates very fast so that even large clusters move as synchronized as small ones.
In order to evaluate the stability of the platoons, i.e., identify stable moving structures, the cross-correlation between the minute averaged velocities at the detectors D3 and D4 on the A1 (Fig. 3.7) is calculated. If the platoons were stable, the order of the vehicles passing a detector would remain unchanged leading to a strong correlation of the velocity

[4]This value should be of the order of the maximum of the time-headway distribution, i.e., about 1 s.

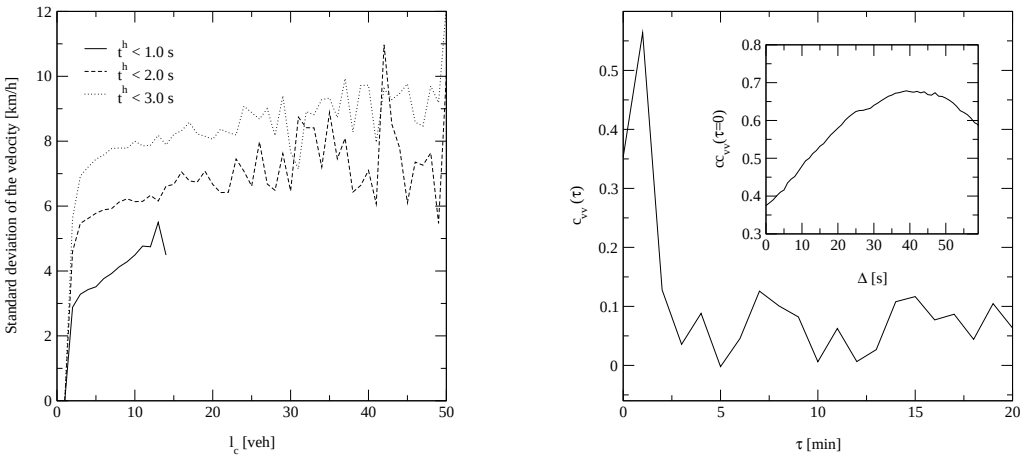

Figure 3.7: Left: Average standard deviation of the mean velocity of the vehicles in a cluster of length l_c on the left lane at detector D1 on the A3 on the 04-28-2000. Right: Cross-correlation between the minute averaged velocities at the detectors D3 and D4 of the left lane on the A1 on the 08-10-2000. The inset shows the cross-correlation for $\tau = 0$ of the velocity time-series at D4 and the by Δ seconds shifted velocity time-series at D3.

time-series. Vehicles on the left lane need about 30 s to drive from $D3$ to $D4$. As one can see, there is indeed a strong correlation of both sites at $\tau = 1$ min, indicating that the lifetime of the platoons may have large values, and moving structures can be identified even in free flow. The analysis of single-vehicle data allows to specify the lag between the two time-series by varying the displacement of the two time-series continuously. The starting point of the averaging interval of the time-series at D3 is shifted by Δ seconds and then, the cross-correlation of the two signals is calculated. If the two time-series match, the cross-correlation would show large values at $\tau = 0$. Hence, it is possible to locate the maximal correlation which corresponds roughly to the average travel time $\Delta_{\max}$ given by 1150 m/150 km/h $\approx$ 28 s (see inset of Fig. 3.7).
As mentioned before, the third data set provides information about the signal the inductive loop measures from each car. Therefore it is tried to identify the moving structures of free flow traffic, not only on the minute averaged scale but also on the single-vehicle scale. Unfortunately, the consideration and comparison of the vehicles' electric signal at both detectors fails for two reasons. First, the electric signal differs only slightly from car to car. Second, even on the right lane the sequence of cars changes due to lane changes and overtaking maneuvers. As a consequence, the number of vehicles on one lane is not conserved so that even the cumulative number of vehicles passing a measurement section cannot be compared [15]. Therefore an explicit identification of a vehicle at both measurement locations was difficult and made the calculation of the travel-time distribution impossible.
In [110] it was shown that in free flow traffic the correlation of the average velocity between different lanes is negligible. However, this result is contrasted by the analysis of the velocity time-series. In Fig. 3.8 is depicted the cross-correlation between the detrended

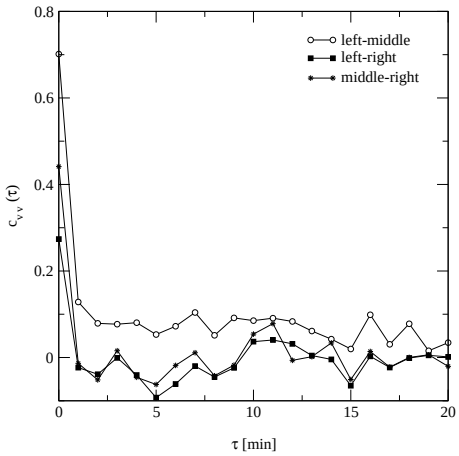

Figure 3.8: Cross-correlation between the minute averaged velocities on the three lanes on the 04-28-2000 at detector D1 on the A3. Note, that the velocity time-series was detrended by a linear fit.

average velocities on lane i and lane j. Obviously, there are strong correlations between the lanes, especially neighboring lanes are more correlated than the left with the right lane. Lane changes lead to a strong coupling between the lanes while the right lane is somehow decoupled from the other two, due to the large amount of trucks. These lane changes are forced by the absence of a speed limit that may explain the differences to the results of [110] where a speed limit was in effect. As a result, daily fluctuations of the mean velocity and therefore of the flow are served first by the left and the middle lane, while the flow of the right lane does not change significantly in the free flow regime.

3.3 Synchronized traffic

Synchronized traffic can be characterized by a large variance in flow and density measurements and a velocity that is considerably lower than in free flow traffic, while the flow can show large values (Fig. 3.9). Although the minute averaged velocity is larger compared to a wide jam, the analysis of the single-vehicle data reveals the existence of vehicles with velocities smaller than 10 km/h, that is vehicles at rest were measured [69].
In contrast to free flow, the time-headway distribution shows a non-trivial dependence on the density (Fig. 3.9). While the maximum of the distribution is shifted to larger values (≈ 1.3 s) and the variance is reduced, small time-headways do still exist. The probability of these small time-headways decreases with increasing density whereas the distribution in free flow can simply be rescaled by the density for small times. Note that the distribution was calculated by the consideration of all days of the data set with synchronized traffic.
Compared to free flow traffic, the length of clusters with small time-headways is decreased significantly (Fig. 3.10). The increased density in the synchronized regime is therefore responsible for the dissolution of the large platoons of the free flow regime. Moreover, due to the fact that the velocity of the cars is now determined by the available space rather than by the desired velocity, the probability of cars piling up behind a slow car is drastically

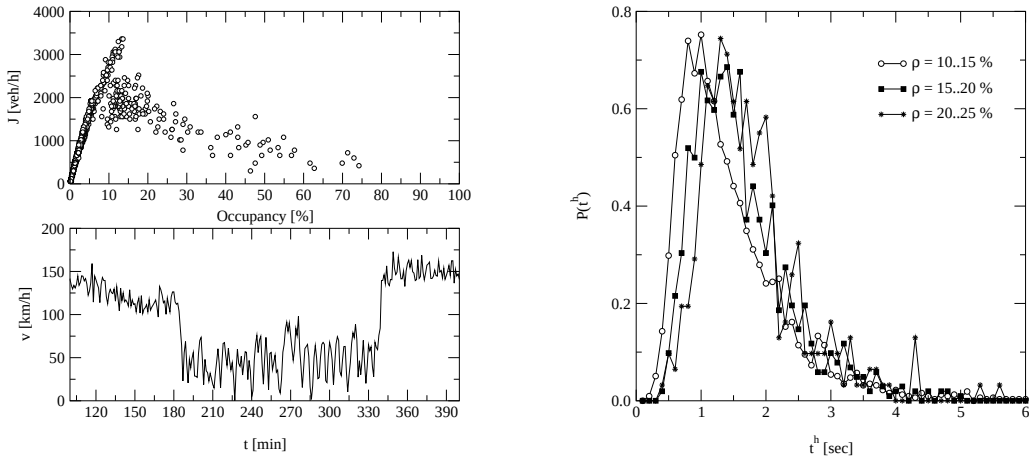

Figure 3.9: Left: Fundamental diagram and time-series of the velocity on the 05-11-2000 of the left lane at detector D1 on the A3. Right: Time-headway distribution in the synchronized regime for all days of the left lane at detector D1 on the A3.

reduced. Now, safety reasons require larger distances to the preceding vehicle, in order to prevent braking maneuvers. Note that large clusters with time-headways larger than 2 s between the vehicles are obtained since the mean time-headway has the same order of magnitude.
Nevertheless, strong correlations of the velocity of the vehicles can be measured, while the time-headway and the distance-headway are only weakly correlated (Fig. 3.10). Thus, although the velocity of succeeding vehicles is strongly synchronized, their gaps can vary considerably. As a result, platoons cannot be recognized.
Also for the velocity distributions, significant differences to free flow traffic are found. In synchronized traffic small velocities have, compared to a Gaussian distribution, a much higher weight (Fig. 3.11). The form of the velocity-distribution is probably a consequence of the accelerating and braking vehicles. This result is of special importance for some macroscopic models of traffic flow that assume Gaussian distributions of speeds, clearly incompatible with the empirical findings.
As shown in [110], the velocity-headway curve gives information about the average velocity of the vehicles at a given headway. In the free flow regime, large velocities are reached even for very small distances, but in synchronized traffic the asymptotic velocity is reduced considerably (Fig. 3.4). Again, the velocity-headway curve was obtained by averaging over all days with synchronized traffic. Since the vehicles drive slower than the gap allows, the gap usage is only suboptimal. Moreover, the velocity of a vehicle at a given distance depends strongly on the traffic density. The larger the density, the lower the velocity which allows the driver to anticipate breakdowns.
The transition from free flow to synchronized traffic is characterized by the synchronization of the speed on different lanes and a sharp drop of the velocity. This synchronization is a result of lane changes in order to align the density of the lanes [19, 73, 79] rather than a consequence of the difference between the maximum velocities of the vehicles.
In Fig. 3.11 the time-series of the velocity measurements for the three lanes is shown.

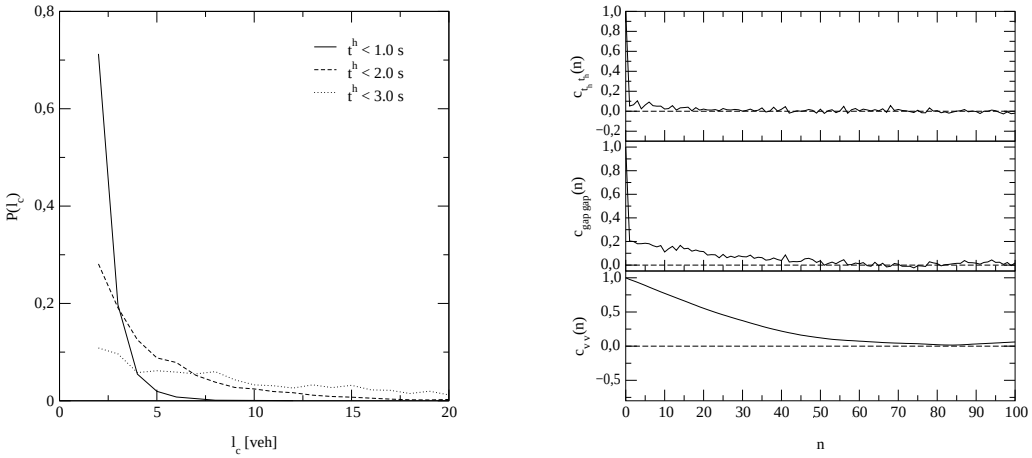

Figure 3.10: Distribution of the cluster length for different time-headways (left) and auto-correlation of the single-vehicle data in the synchronized state of the velocity and the time- and the distance-headway (right) of the left lane at detector D1 on the A3 on the 05-11-2000.

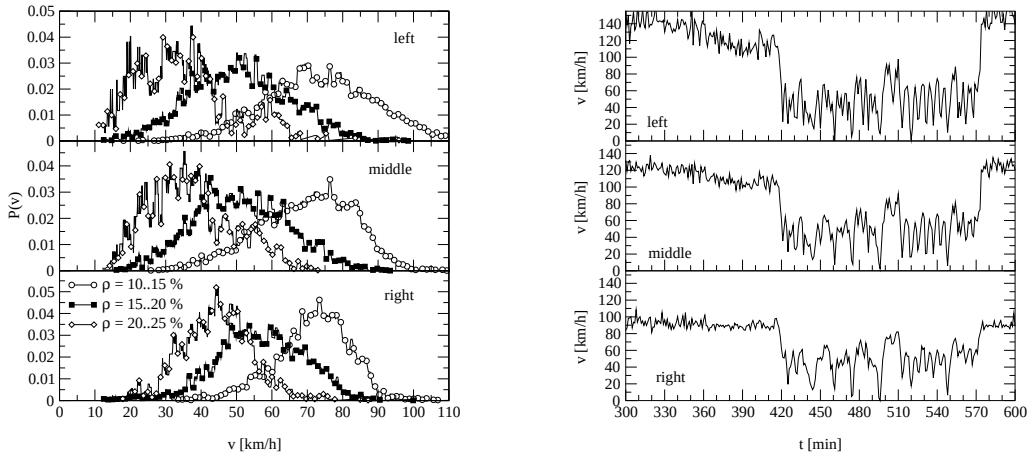

Figure 3.11: Left: Corrected distribution of the velocity in the synchronized regime. Right: Velocity time-series at detector D1 on the A3 on the 05-11-2000 for all three lanes.

A slow decrease of the average velocity on the left and on the middle lane can be seen until a sharp drop of the velocity occurs. Obviously, the breakdown happens at the same time for all three lanes. In contrast to the velocity, the density difference between the lanes decreases continuously and completely vanishes at the transition (Fig. 3.12). The synchronization of the lanes therefore happens continuously.
The calculation of the cross-correlation between the velocities, the densities and the flows

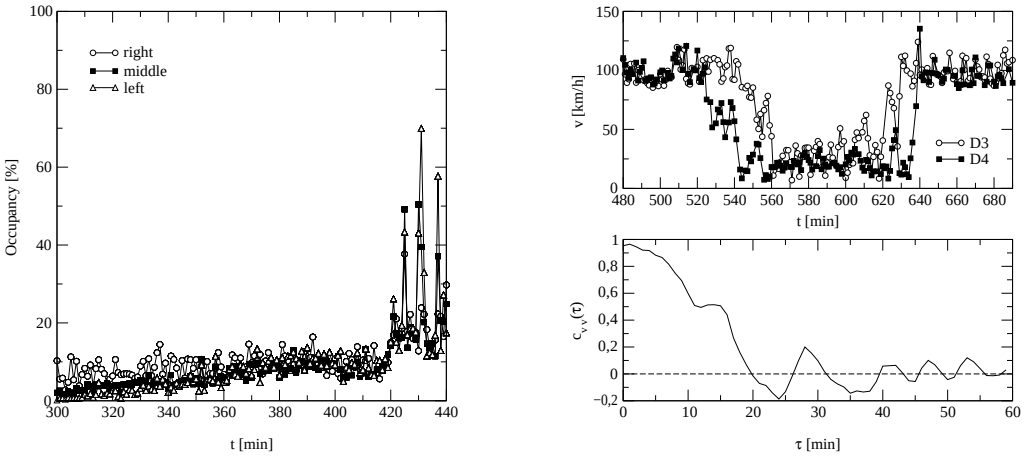

Figure 3.12: Left: Occupancy time-series of the three lanes at detector D1 on the A3 on the 05-11-2000. Right: Cross-correlation (bottom) between the velocity time-series (top) of synchronized traffic of the middle lane on the 02-20-2001 at the detectors D3 and D4 on the A1.

on the three lanes reveals that the lanes are strongly correlated, e.g., synchronized. As a consequence of this synchronization, the distribution of the velocity, the distance-headway and the time-headway are nearly the same for each lane. Thus the basic driving behavior in synchronized traffic is determined neither by the density nor by the lane but depends only on the traffic state.
Again, the cross-correlation analysis of the velocity time-series between the detectors D3 and D4 on the A1 allows the identification of moving structures (Fig. 3.12). The difference in the life-time of the synchronized states at each location suggests the existence of a bottleneck far upstream of D4 where a transition from free flow to synchronized traffic has occurred. As an indication for the stochasticity of the jam formation mechanism, velocity fluctuations increase with the distance to the bottleneck, finally leading to a pinch region with small jams. The propagation of these small jams leads to a small decay of the cross-correlations of the order of magnitude of 10 min which is about the period of the jam emergence at one measurement location. However, the upstream velocity of these small jams cannot be determined due to their continuous excitation and extinction.

3.4 Wide moving jams

In contrast to free flow and synchronized traffic, wide moving jams are moving structures that are bounded by two fronts where the vehicle speed changes considerably. The flow and the velocity inside the wide jam are negligible whereas the density has large values (Fig. 3.13). These large values of the density can be traced back to a large number of vehicles that passed the detector rather than to a single car at rest that occupies the detector for a long time. This is confirmed by shifting the time for 60 s the minute averaging starts and then calculating the mean density of these values. It turns out that the mean density did not decrease.

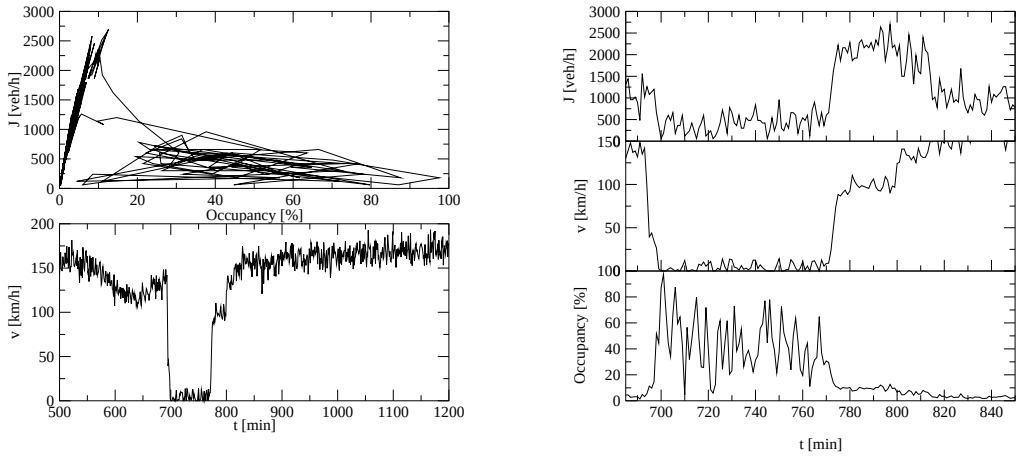

Figure 3.13: Fundamental diagram and velocity time-series (left) and time-series of the flow, the velocity and the occupancy (right) of the left lane on the A3 at detector D2 on the 04-15-2000.

In the fundamental diagram the wide jam can be identified by a triangle structure at large densities and small flows (Fig. 3.13). Two effects have to be taken into account in the interpretation of the data for wide jams: 1) Wide jams are not compact in the sense that cars are piled up bumper-to-bumper, but there can still exist relatively large gaps inside. These gaps lead to small values of the density and the flow. 2) Standing vehicles can block the detector for a certain time. This results in large densities but small flows.
The characteristics of a wide jam are the upstream moving velocity and the outflow from the jam if free flow is formed in the outflow. As one can see in Fig. 3.13, the transition from the wide jam to free flow is accompanied by a jump of the velocity to values lower than in free flow traffic, while the density and the flow are considerably larger (Fig. 3.13) determining J_{out} and ρ_{out} [73] to be 2200 veh/h and 10%. In addition, the difference of the outflow from a jam to free flow traffic decreases from the left to the right lane due to the decreasing average velocity.
Inside the jam, the velocity and the flow are negligible. Since vehicles can only move due to the propagation of holes, the velocity inside a wide jam is distributed only in a very small range (Fig. 3.14).
Note that the cut-off is due to measurement restrictions, e.g., velocities smaller than 10 km/h are not detected. As mentioned before, the calculation of the headways is only correct under the assumption that the velocities of two consecutive vehicles do not change significantly. However, relatively large values of the time and the distance headway become visible (Fig. 3.14). This fact can be explained by gaps within the jam. Hence, the wide jam is not compact, but gaps allow the movement of the vehicles.
If vehicles with a velocity smaller than 10 km/h pass the detector, the velocity is not detected but instead of the length of the vehicle, its time blocking the detector is given. This time, the occupancy time Δt_n allows to estimate the time, a car n at rest needs to accelerate [5]. In Fig. 3.14 the distribution of the occupancy time is shown. Obviously, a

[5]Since it is possible that the vehicle has to stop at the detector the assumption of a constant velocity is

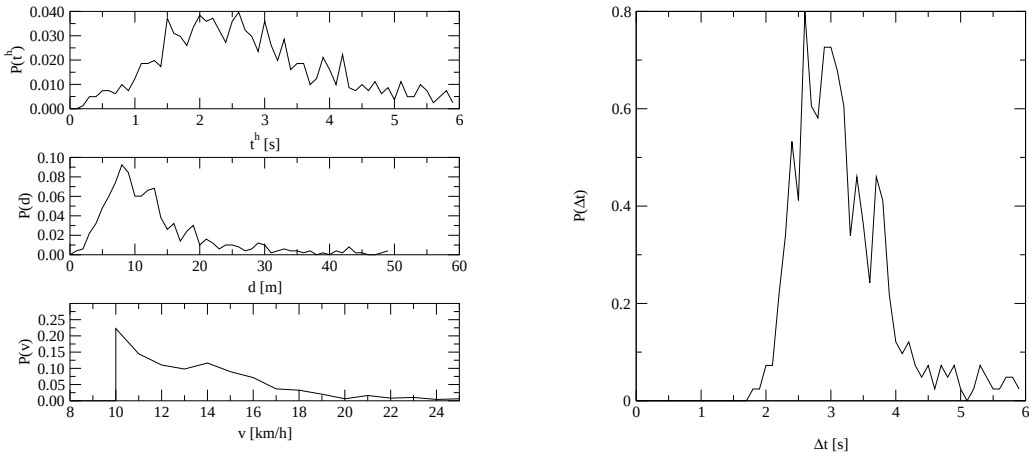

Figure 3.14: Left: Distribution of the time and the distance headway and the velocity in a wide jam for the left lane on the A3 at detector D2 on the 04-15-2000 and at detector D1 on the 05-02-2000. Right: Distribution of the time the detector is occupied by a car with a velocity smaller than 10 km/h in a wide jam.

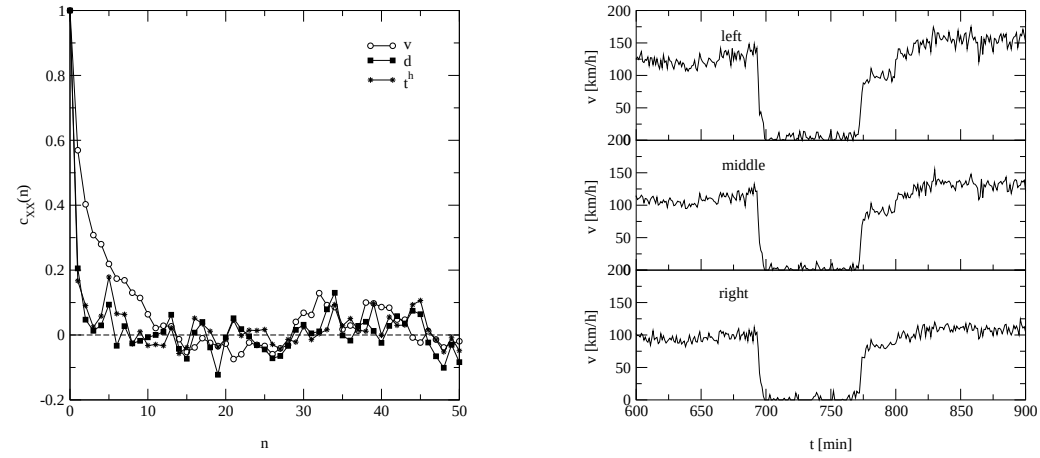

Figure 3.15: Autocorrelation of the single-vehicle data of the velocity and the time- and the distance-headway in a wide jam (left) and time-series of the velocity for the three lanes (right) on the 04-15-2000 at detector D2 on the A3.

vehicle needs a minimal time of about 2 s to accelerate. As a characteristic property of a wide jam [67], this time determines (including the density inside the jam) the escape rate from a jam and thus its outflow.
As a consequence of the gaps inside the jam, a stop-and-go pattern forms that leads to

no longer valid. Thus, the calculation of the time-headway is not possible.

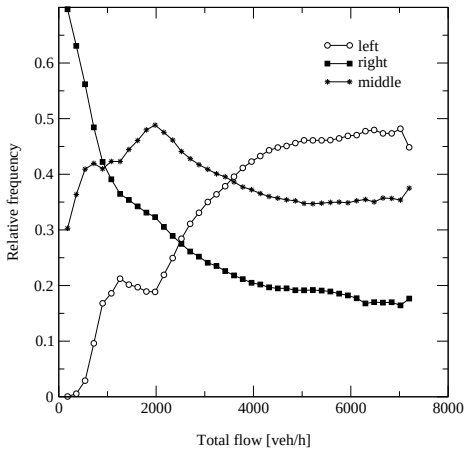

Figure 3.16: Distribution of the total flow on the three lanes.

an uncorrelated movement of the vehicles. However, in contrast to the autocorrelation function of the time-headway and the distance-headway, the correlation of the single-vehicle velocity decays slower (Fig. 3.15). Thus, weak correlations between the vehicles on very short length scales exist that can be traced back to the successive acceleration of stopped vehicles.
In analogy to synchronized traffic, the transition from free flow traffic to wide jams is accompanied by an alignment of the densities on the different lanes. In contrast to the transition from free flow to synchronized traffic, the velocity difference between the lanes does not decrease, indicating that the breakdown happens due to a large perturbation. Nevertheless, the breakdown of the velocity time-series can be observed at the same time on all lanes, which is a consequence of the synchronization of the lanes.
As the next step, the so-called lane-usage inversion is analyzed. The lane-usage inversion is a special phenomenon observed on German highways [130] and concerns the distribution of the total flow on the lanes. For low densities, nearly all the flow can be measured on the right lane. However, above a certain density, the inversion point, most of the flow can be found on the left lane rather than on the right lane. This special observation can be explained by the legal restrictions of highway traffic in Germany. Since the left lane is the designated fast lane, vehicles must drive on the right lane where overtaking is forbidden. As a consequence, at larger densities, cars keep on moving on the left lane in order to avoid being trapped behind a slow car on the right lane. Thus, more and more flow can be found on the left rather than on the right lane. This behavior is contrasted by observations on American freeways [17, 39].
In Fig. 3.16, the distribution of the flow on the three lanes averaged for the whole data set of the A3 is depicted. In contrast to observations of two-lane traffic, in three-lane traffic three inversion points are visible. At a flow of about 1000 veh/h, the weight of the distribution is shifted from the right to the middle lane. At a total flow of about 2500 veh/h, the second inversion point is reached, and more flow can be found on the left than on the right lane. Finally, at flows larger than 3500 veh/h, the share of the flow is larger on the left than even on the middle lane.

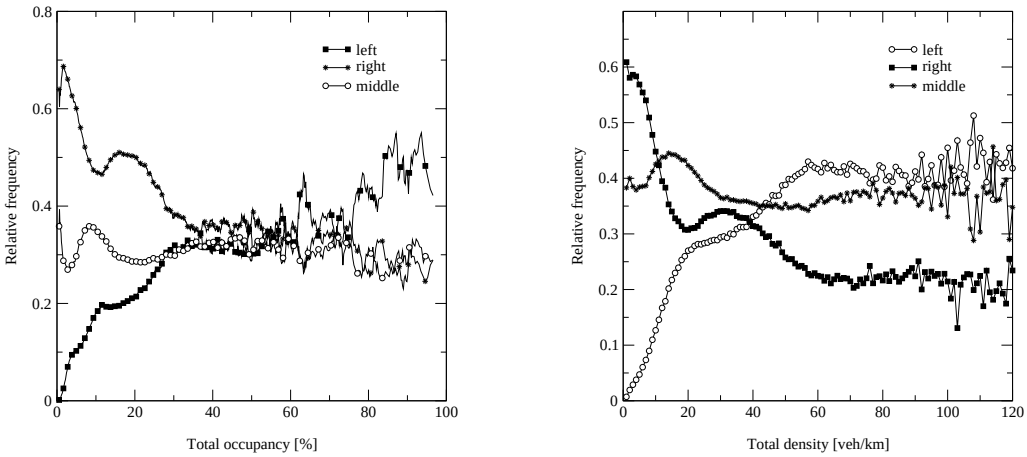

Figure 3.17: Left: Distribution of the total occupancy on the three lanes. The data were smoothed by a running average. Right: Distribution of the total spatial density on the three lanes.

In contrast to the flow distribution, the distribution of the total occupancy shows no inversion points. As mentioned before, the transitions from free flow to either synchronized traffic or wide jams is accompanied by an alignment of the density as shown in Fig. 3.17. Right before the transition, the density is evenly distributed on the three lanes. For all densities there is a negative density gradient from the right to the left lane. With increasing density, the difference between the lanes decreases, but there are no densities where there are more vehicles on the left than on the right lane. However, as mentioned in section 3.1, occupancy gives the percentage of the measurement time the detector is covered by vehicles. Therefore, the slower the vehicles, the larger the occupancy since slow vehicles occupy the detector for a longer time than fast vehicles. In order to estimate the spatial density, it is necessary to measure the mean length of the vehicles on the individual lanes. With the values $\mathcal{L}_{\text{left}} = 4.25$ m, $\mathcal{L}_{\text{middle}} = 4.57$ m and $\mathcal{L}_{\text{right}} = 8.3$ m the density can be calculated via equation (2.9).
As one can see in Fig. 3.17, there is indeed a lane-usage inversion. At densities well below a certain point, more vehicles are on the left than on the right and the middle lane, leading to a negative flow gradient from left to right. In addition, the cross-over of the density distribution occurs analogously to the flow distribution at three inversion points. As a consequence of the large amount of trucks on the right lane, the left and the middle lane show nearly the same lane occupancy which is considerably larger compared to the right lane. This fact is another indication for the decoupling of the right from the left and the middle lane.
Thus, the lane usage inversion can on one hand be traced back to differences of the average velocity between the lanes that lead to larger flows from right to left, and on the other hand to an asymmetric distribution of the vehicles on the lanes (the flow inversion can also be observed on highways with speed limit).

3.5 Conclusion

The analysis of single-vehicle traffic data leads to a more elaborated microscopic picture of highway traffic. In the free flow state, correlations between the vehicles are only visible on scales smaller than one minute. The correlations result from platoons, i.e., clusters of cars driving bumper-to-bumper with very small time-headways. Within these clusters, the vehicles are driving with nearly the same velocity, leading to a large temporal stability of the platoons. With increasing size of the platoons a larger distance between the vehicles inside the platoon can be observed.
In contrast to highways without speed limit, with speed limit drivers tend to drive with larger temporal distance, i.e., the probability of very small headways is reduced considerably, and the maximum of the time-headway distribution is shifted towards larger values. This may indicate that speed-limits lead to a reduction of accidents. But even more efficient than that would be the reduction of the number of drivers driving with time-headways comparable to their reaction time, e.g., by equipping cars with devices that adjust automatically the distance to the leading car.
Another remarkable effect that can already be observed in the free flow regime is the synchronization of speeds on the different lanes, which was predicted by different simulation studies [19, 79].
The velocity distributions that are important as an input for macroscopic traffic models [42], exhibit the expected Gaussian shape for densities of $5 - 10\%$. Surprisingly this is not true for very low densities. In these cases the distribution functions show a slight asymmetry with an increased weight of large speeds.
The synchronized traffic state is known to be characterized by increased fluctuations, e.g., of the velocity time series, compared to free flow traffic. On a microscopic level, these fluctuations influence the time-headway distributions on short time scales. The short headways are systematically suppressed, and the maximum of the distributions is shifted towards larger headways. This effect may be explained by the tendency of drivers to avoid frequent accelerations and brakings [81]. Other consequences of the larger velocity fluctuations are the more rapid dissolution of the platoons in synchronized traffic and the much higher weight of small velocities. The low speed part of the velocity distribution is probably governed by acceleration and braking vehicles.
Wide jams can be identified by a triangular shape in the fundamental diagram. Since they are not compact, the transportation of holes leads to small flows at small densities. The analysis of the time a vehicle at rest covers a detector allows to estimate its acceleration time. This time determines the outflow from a jam and is characteristic for wide jams. The result of about 2 s confirms the value found in [67].
The transition from free flow to either synchronized traffic or wide moving jams is accompanied by a continuous alignment of the density on the different lanes. The breakdown of the velocity happens simultaneously, which is a consequence of the synchronization of the vehicle's speed on the lanes.
Empirical studies reveal that on German two-lane highways the flow is distributed asymmetrically on the lanes. This lane usage inversion is a result of the asymmetric distribution of the vehicles on the lanes and can be found even on three-lane highways. It is increased by a negative velocity gradient from the left to the right lane on highways without speed limit.
The analysis confirms the basic results of former empirical studies [110, 133]. In particular, the characteristics of the time-headway distribution and the velocity-distance curve have been found in both data sets. The new data allow to clarify an open question about the

occurrence of peaks in the time-headway distribution [110], that are most likely an artifact of the internal data handling of the inductive loops. The present results reveal that a peak at a headway of 1.8 s does not exist.
Finally, it has also to be stressed that the different traffic states that have been identified by means of a spatio-temporal analysis of time-averaged data differ equally well with respect to their microscopic structure. Hence, this coherence between microscopic and macroscopic empirical analyses supports the validity of the classification scheme.